Biosensors and Bioelectronics 138 (2019) 111310

Contents lists available at ScienceDirect

Biosensors and Bioelectronics

journal homepage: www.elsevier.com/locate/bios

# A novel disposable self-adhesive inked paper device for electrochemical sensing of dopamine and serotonin neurotransmitters and biosensing of glucose

Luiz Otávio Orzari[a], Rafaela Cristina de Freitas[a], Isabela Aparecida de Araujo Andreotti[a,b], Alexandre Gatti[c], Bruno Campos Janegitz[a,*]

[a] Department of Nature Sciences, Mathematics and Education, Federal University of São Carlos, 13600-970, Araras, SP, Brazil
[b] Center for Exact Sciences and Technology, Federal University of São Carlos, 13560-000, São Carlos, SP, Brazil
[c] FlackTek Inc, 1357-4290, São Carlos, SP, Brazil

ARTICLE INFO

*Keywords:*
Disposable electrode
Point-of-care
Self-adhesive paper
Neurotransmitter
Glucose

ABSTRACT

In this work, we detail the progress of a novel electrochemical disposable device, which has a relatively low cost and easy production, with a novel conductive ink, that consists of graphite and automotive varnish mixture, deposited over a self-adhesive paper, granting an easy production with relatively low cost. The electrode surface was characterized by scanning electron microscopy, X-ray powder diffraction and Fourier transforms infrared and Raman, cyclic voltammetry and electrochemical impedance spectroscopies. In addition, the proposed electrode was applied for individual electrochemical determination of dopamine and serotonin. The device achieved a linear response between 30 and 800 μmol $L^{-1}$ and a limit of detection (LOD) of 0.13 μmol $L^{-1}$, by square wave voltammetry for dopamine and a linear range from 6.0 to 100 μmol $L^{-1}$, with a LOD of 0.39 μmol $L^{-1}$, by differential pulse voltammetry for serotonin. Later, the working electrode was modified with glucose oxidase and dihexadecyl phosphate film in order to obtain a biosensor. At this stage, CV was applied to detect glucose in the range of 1.0–10 μmol $L^{-1}$ and LOD of 0.21 μmol $L^{-1}$. By three different techniques and analytes, the sensoring and biosensoring processes presented high reproducibility. The proposed adhesive electrode is easy to prepare, disposable, within non-restrictive nature, which allows an approach of a new device for electrochemical sensing and biosensing.

## 1. Introduction

The recent interest in ridding patients of the dependence on a sophisticated laboratory and more advanced and expensive technologies for a diagnosis has been moving global science, which, allied to innovative advances, such as the use of miniaturized devices, wireless communication, and nanomaterials, prove the point-of-care (POC) potentiality. (Goldstein, 2003; Schultz, 2001; Syedmoradi et al., 2017; Zarei, 2017). In this context, they present attractive qualities, such as practicality, ease of use, relatively low cost and short time response, while also require minimal equipment operation and specific knowledge. As one of the major uses of such devices is the monitoring of diseases that requires routine tests, such as diabetes, POC devices can be performed with a focus on the patient, increasing the healthcare system efficiency (Goldstein, 2003; Schultz, 2001; Syedmoradi et al., 2017; Zarei, 2017). Another advantage of POC devices is the acceptance of common and disposable materials, favoring a more sustainable approach (Janegitz et al., 2014; Johari-Ahar et al., 2018; Lamas-Ardisana et al., 2018; Xu et al., 2018). Some recent works have been proposed by using disposable inert substrates for electrochemical devices (Dunn, 2003; Mittal, 2003; Orzari et al., 2018; Tortorich et al., 2018), with a relatively lower cost than conventional electrodes with similar performance. Nowadays, adhesives are commonly found in our environment, being frequently attached to cellulose substrates, as stamps, stickers, many everyday tapes and even medical plasters (Negash et al., 2015; Purushothama et al., 2018; Sharp and Burkitt, 2015). In this regard, the adhesive paper is an interesting alternative for different applications (Dunn, 2003; Mittal, 2003). Paper is a substrate for novel electrochemical systems that has been gaining attention in the last years (Ge et al., 2012; Lee et al., 2018; Tortorich et al., 2018; Wang et al., 2017), which presents biocompatibility and biodegradability. Therefore, adhesive papers can increase the field application, as no set place is

* Corresponding author.
*E-mail address:* brunocj@ufscar.br (B.C. Janegitz).

https://doi.org/10.1016/j.bios.2019.05.015
Received 4 February 2019; Received in revised form 2 May 2019; Accepted 6 May 2019
Available online 09 May 2019
0956-5663/ 

needed for the measurement, also bringing all advantages of regular paper.

Being highly known for its conductive properties, graphite is a superposition of $sp^2$ carbon sheets, which produces interesting anisotropic effects. In graphite, the carbon interactions may be limited between planes, conferring some resistivity, being an excellent thermal and electrical insulator (Fukushima et al., 2006; Pierson, 2012; Tian et al., 2013). Also, it is easily sheared, as the interlaminar strength is considerable low. However, due to its σ bonds, graphite has admirable electrical conductivity at laminar planes, being even higher than some metals (Fukushima et al., 2006; Pierson, 2012; Tian et al., 2013). Also, its whole structure can present vacancies, dislocations and other structural imperfections, which could lead to a lower density, allowing it to be considered one of the lighter refractories (Khomenko et al., 2008; Li et al., 2005; Pierson, 2012). These properties, along with its chemical inertia (Pierson, 2012), favor the development of electrodes (Negash et al., 2015; Purushothama et al., 2018; Sharp and Burkitt, 2015) and conductive polymeric inks (Grisales et al., 2016; Phillips et al., 2017), in a raw proportion of up to 50% (1:1 graphite:polymer) of final composition, without any electrical conduction loss (Pekarovicova and Fleming, 2005). The literature has been presenting a range of works in which carbon-based inks are used in the development of different electrochemical systems (Jaiswal and Tiwari, 2017; Sharp and Burkitt, 2015).

As proof of concept, we applied the device towards the individual detection of dopamine and serotonin, two of the most electrochemically well acknowledged and important catecholamines in mammals, mainly due to their connection with several behavioral dependence and Parkinson disease (Baccarin et al., 2017; Berridge and Kringelbach, 2013; Fox et al., 2009; Goldstein, 2003; Iversen et al., 1977; Mayeux et al., 1984; Schultz, 2001; Sharma et al., 2018; Vyazovskiy et al., 2007). After, we modified its surface with glucose oxidase (GOx), demonstrating the sensitive detection of glucose, an essential monosaccharide, that has substantial impact in the brain behavior, as well as its discrepant rates are the cause of diabetes (Arslan et al., 2011; Blair, 2016; Cryer, 2016; Dwier, 2002; Janegitz et al., 2011; Pisoschi, 2012; Wang and Lee, 2015).

## 2. Experimental

### 2.1. Chemicals and reagents

All reagents used in the present work were purchased from Sigma-Aldrich (Germany) and/or Fluka (Brazil), in analytical grade. Ultrapure water (Megapurity, USA), with resistivity > 18 MΩ cm, was used for the preparation of all electrolytic solutions. Dopamine and serotonin were purchased from Sigma-Aldrich (Germany). The graphite powder (Gr) used was obtained from Fischer Chemical (USA), and the ink polymeric vehicle was the automotive varnish from Sherwin-Williams (Brazil), Lazzudur 2 K Auto Brilho (AV). For electrochemical characterization of the device, as well as dopamine detection, 0.1 mol $L^{-1}$ phosphate buffer (Sigma-Aldrich, Germany) (PB) solution (pH 6.1) was used as supporting electrolyte. Glucose biosensing was performed in 0.05 mol $L^{-1}$ PB solution with pH 7.0 for optimal glucose oxidase (Sigma-Aldrich, Germany) (78 units per electrode) activity.

### 2.2. Apparatus

A Tescan VEGA-3 LMU microscope was used to perform the scanning electron microscopy (SEM), with an accelerating voltage of 10 kV, in low vacuum mode with 50 Pa. Fourier transform infrared spectroscopy (FTIR) was carried out with a Tensor II spectrophotometer (Bruker), in 4.0 $cm^{-1}$ resolution and transmittance mode from 400 to 4000 $cm^{-1}$. Raman spectra were obtained using a B&W Tek *i*-Raman BWS 415–785H spectrometer, with an excitation laser of 785 nm. A B&W Tek microscope BAC151A, coupled to the spectrometer was used, with 3.5 $cm^{-1}$ spectral resolution, in the spectral range of 0.5–2500 $cm^{-1}$, the acquisition time of 120 s, and laser power of 70 mW. The x-ray diffraction (XRD) was performed by a Miniflex II x-ray diffractometer (Rigaku), with a CuKα radiation source (λ = 0.15406 nm), from 3° to 90° angular recording range, with a step of 0.02° and 10° $min^{-1}$ analysis time. All electrochemical measurements were performed with an Autolab PGSTAT204 (Eco Chemie) potentiostat/galvanostat (with FRA32M module) managed by NOVA 2.1.3 software. An 827 pH-meter (Metrohm) was used for pH measurements. The conductive ink was mixed and milled with a dual asymmetric centrifuge (DAC) SpeedMixer™ Dac 150.1 FVZ-K (FlackTec Inc) and the electrodes were cut with a cutting printer (Silhouette, Cameo 3).

### 2.3. Preparation of the conductive ink

In the ink technology field, it is common to prepare inks by suspending pigments in a resin/polymer vehicle. For the electrically conductive materials, specific components are added to the formulation, granting the desired aspects. Here, as well as the colorant, Gr was used as the conductive material. Therefore, 7.2 g of Gr was added to an aliquot of 18 g of AV, corresponding to 30% of the desired final ink mass. Afterward, the suspension was mixed for 3 cycles of 3500 rpm for 90 s in SpeedMixer. It is important to highlight that this mixer has a dual asymmetric centrifuge that milling, mixing and consequent heating of particles. Therefore, there was no need a polymeric curing agent, and the ink could easily solidify at room temperature.

### 2.4. Preparation of the disposable electrode, modification, and electrochemical measurements

Fig. 1 illustrates the disposable device (Gr-AV) preparation. Firstly, the graphite ink is applied on an adhesive paper sheet, respecting the edges of the cutting printer (Silhouette, Cameo 3), which is used to cut the format of the devices. Then, it was waited 40 min for the ink to dry. Succeeding, the excess is removed and properly discarded, resulting in a sheet full of disposable devices with working (Ø = 4.5 mm diameter), counter and reference electrodes, ready to use. A video of this process is also available in the supplementary data (Video 1). For the biosensor (Figure 1B), 10 μL of GOx and dihexadecyl phosphate (DHP, 1.0 g $L^{-1}$) solution was previously prepared and cast on the working electrode surface and let dry overnight at 10 °C.

Supplementary video related to this article can be found at https://doi.org/mmcdoino.

To execute the electrochemical measurements, the device was adhered to a polyethylene terephthalate substrate and later to a connector previously built by the group (Orzari et al., 2018), as observed in Fig. S1A (supplementary material). 70 μL of supporting electrolyte and analyte solution was cast on the disposable system and 10 s of waiting time was standardized in dopamine analysis, due to the absorptive nature of paper. The waiting time for glucose biosensing was 60 s, aiming the enzyme reaction and to standardize the water absorption problem.

### 2.5. Detection and samples preparation

As previously mentioned, both analytes have interesting impacts in modern human society: dopamine has a well-known relation to human desire, behavior and many neurological disorders; and glucose is a biomarker for diabetes in its metabolism process. In this regard, all detections were performed by addition and recovery method, in synthetics urine, saliva and saline samples. The synthetic samples were prepared as presented in the literature (Baccarin et al., 2017; Campos et al., 2018; Raymundo-Pereira et al., 2016). The saline solution is a notable biological media, necessary for many optimal biological processes (Kent et al., 1985; Ozawa et al., 2006; Steinbusch et al., 1978) and was also chosen to be a detection media. In addition, all samples

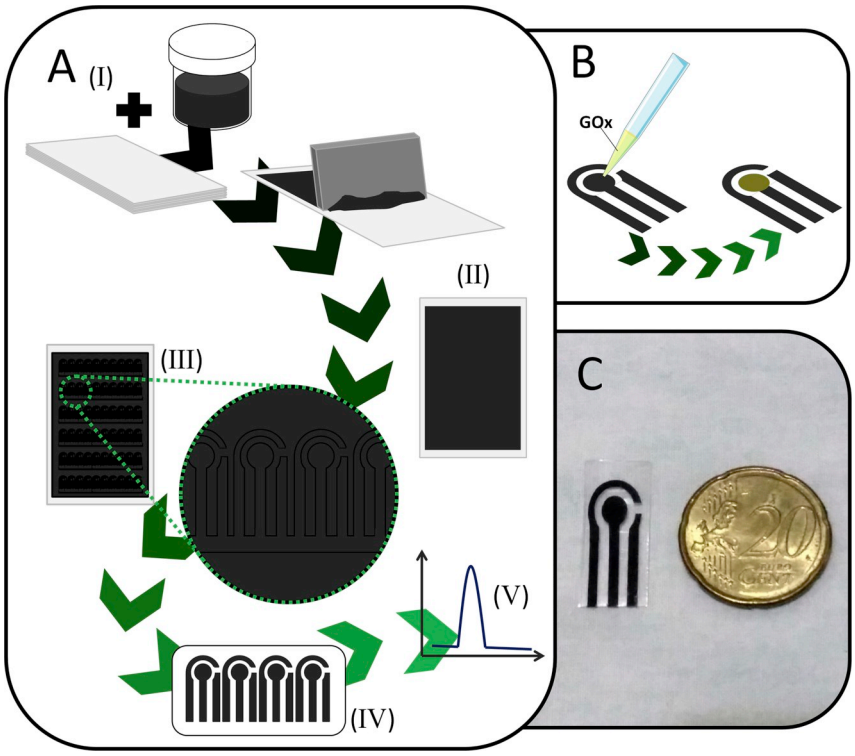


**Fig. 1.** (A) Gr-AV electrode preparation: (I) Conductive ink preparation and application over a self-adhesive paper sheet. (II) After drying for 40 min, the (III) electrodes are printed. (IV) ink excess is removed and the device is ready for (V) electrochemical analyses. (B) The casting of GOx-DHP over the working electrode surface. (C) The device ready to use.

were prepared in PB solution, with optimal pH and ionic strength ($\mu$) (saline samples: 6.1 (Gr-AV) and 7.0 (GOx-DHP/Gr-AV); synthetic urine: 6.1; synthetic saliva: 7.0; all with $\mu = 0.2\ mol\ L^{-1}$) and Table S1 shows all reactants and its concentrations used for each sample, as found in literature (Baccarin et al., 2017; Campos et al., 2018; Raymundo-Pereira et al., 2016).

## 3. Results and discussion

### 3.1. Morphological and electrochemical characterization of the disposable device

Nowadays, there is a great focus on the electroanalytical field to develop novel electrodes structures. This interest is mainly motivated by the possibility of further miniaturization of the system, allowing more practicality and the use of relative cheaper materials. The AV was selected as ink vehicle due to its polymeric composition, great accessibility and relatively low cost. Even though its precise composition is not given by the manufacturers, polyurethane plays a major role in this varnish, which is an interesting compound for application in sensors development. Also, as described, here we present the use of self-adhesive paper as a support for electrodes, and, as a new electrochemical tool, its properties must be known for a better application. Therefore, the self-adhesive device surface was characterized by microscopy and spectroscopy techniques, as shown in Figs. 2–4. Fig. 2 shows the SEM images obtained for the self-adhesive paper sheet (Fig. 2A1-3), the self-adhesive device (Fig. 2B1-3) and the same device with GOx-DHP addition (Fig. 2C1-3). It can be observed the difference between these stages, with the adhesive paper presenting an expected homogeneous fibrous surface being highly rough and porous. This surface is completely changed by the ink, as only graphite associated morphology can be seen in the correspondent image. Then, the casting of GOx-DHP on the working electrode also alters the surface, making it smoother with distributed small enzyme clusters.

Fig. 3A shows the FTIR spectra obtained for the AV (blue line), Gr-AV conductive ink (red line) and Gr (black line). The varnish spectrum presents expected bands, such as the carbonyl stretching at 1730 $cm^{-1}$, the asymmetric stretching of the ester at 1145 $cm^{-1}$, the broadband of O–H stretching and N–H vibration at 3450 $cm^{-1}$, as well as many bands associated with aromaticity, related to a major presence of polyurethane in the varnish composition (Smith, 1982). The bands at 1630 and 1380 $cm^{-1}$, respectively associated with the C=C bonds of the $sp^2$ hybridization and skeletal C–C carbon rings vibrations are found in the graphite spectrum. It is interesting to note that the ink spectrum portraits the same profile as the graphite one. This indicates that not only the paper surface is completely covered, but also that the polymeric part, as well as other organic components, does not interfere in the bulk electrode surface.

Fig. 3B shows the Raman spectra for AV (blue), Gr-AV conductive ink (red) and Gr only (black). Even though the AV spectrum presents a similar profile when compared to polyurethane spectra in the literature (Naumenko et al., 2012; Parnell et al., 2003; Xu et al., 2000), significant shifts can be found. These results are attributed to the several other components in the varnish, which can promote such behavior. Due to limitations of the available equipment, not so normally useful spectra were obtained for Gr and Gr-AV. However, these data also suggest that the dried ink surface is mainly composed by Gr that promotes high conductive characteristics.

XRD measurements were carried out for AV, Gr-AV, and Gr, as shown in Fig. 3C, in order to analyze the crystallinity of these materials, since conductive properties are directly correlated. As observed in the literature (Armelin et al., 2017; Blackwell et al., 1981; Pradhan and Nayak, 2012), polymeric materials have presented amorphous structures with few crystalline phases, because of the non-uniformity of interactions. Therefore, the obtained AV profile corroborated with this, showing a diffused broad diffraction, with a maximum at $2\theta = 17.7°$, as shown in the figure inset. The Gr profile demonstrated a characteristic (Johra et al., 2014; Popova, 2017) (002) plane peak at $2\theta = 26.3$, with a crystal size of 26.96 nm and layer spacing of 1.98 Å. The ink profile showed similarities with the Gr one, but with considerable changes. The plane peak slightly shifts to $2\theta = 26.2$, which presented a higher crystal size, 31.54 nm, and closer layers, with a 1.74 Å spacing. This is attributed to the agglomeration effect and interaction between Gr and AV, by reason of the ink formation process.

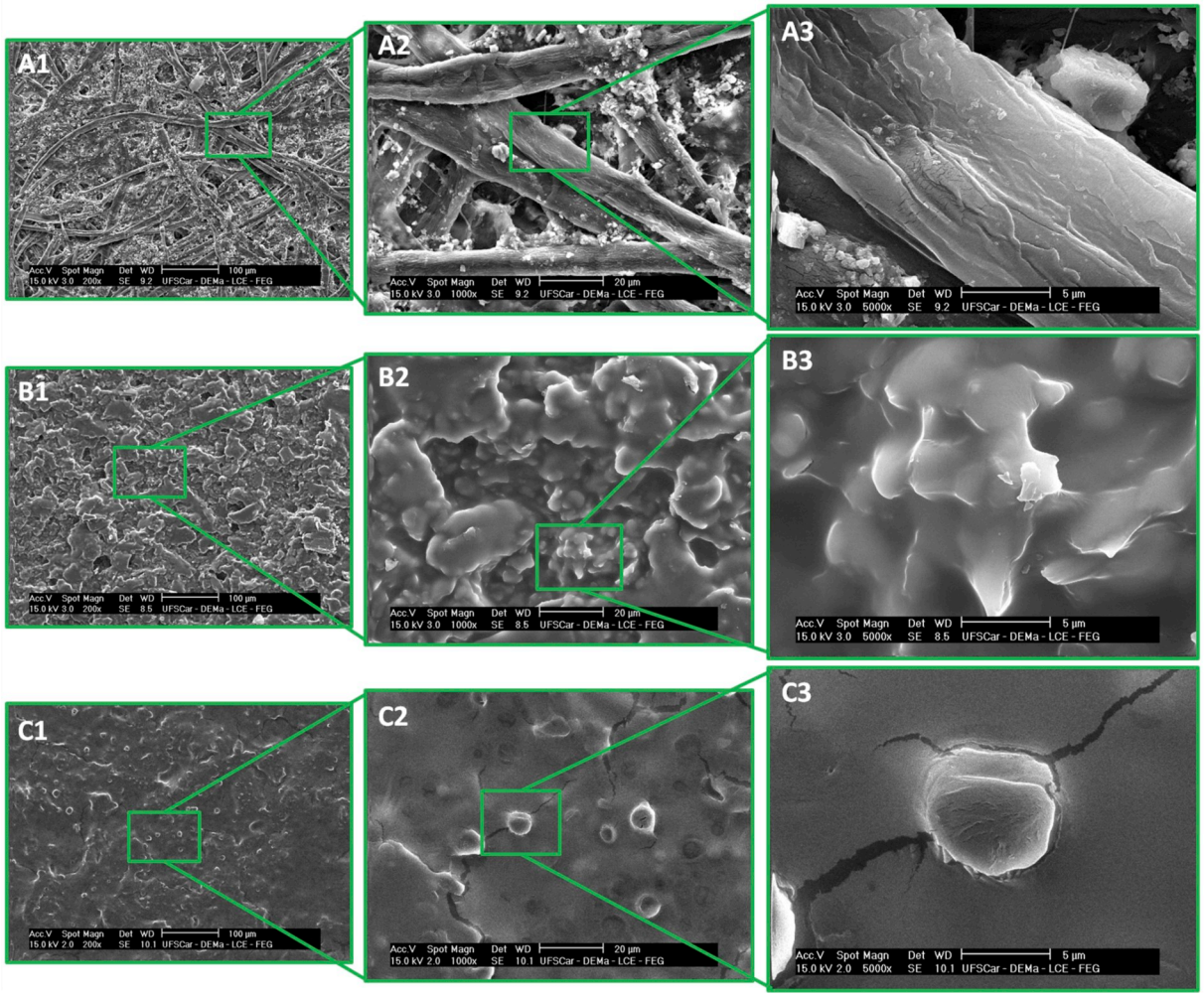


**Fig. 2.** SEM images of (A) self-adhesive paper, (B) Gr-AV and (C) GOx-DHP/Gr-AV at (1) 200, (2) 1000 and (3) 5000 times increase.

Generally, electroanalytical sensors are applied in aqueous media. Consequently, it became necessary, and of great importance, to define the useful working potential window, where water does not suffer electro-induced reactions (Orzari et al., 2018). Fig. 4A shows the cyclic voltammograms obtained by the adhesive sensor in different media: HCl, NaOH, and KCl; maintaining the $\mu$ (all in 0.1 mol $L^{-1}$), at 50 mV $s^{-1}$. A variation in the electrochemical behavior is expected because of the different activity of hydronium and hydroxyl ions (Calegari et al., 2017; Kang et al., 2017). For example, Kang et al. (2017) have studied the effect of water electrolyzation at different pHs by cyclic voltammetry with a copper-based electrode, in which the production of $H_2$ is electrocatalyzed by lowering the pH. In the acidic media, the hydrogen formation can be observed in the proposed electrode, as expected, towards more positive potentials, with the useful region being between −0.45 and 1.3 V. In alkaline media, this potential region was limited between −0.15 and 0.75 V, since the oxygen production is early favored. In neutral media (KCl), by reason of the equivalent presence of water ions, a broader range is expected. However, the non-interfering region corresponded to −0.10 to 1.3 V. Thus, it was possible to observe when lower the pH, the proposed device presented less interference.

To study the electrochemical behavior, Gr-AV electrode was submitted to cyclic voltammetry, at 50 mV $s^{-1}$, in the presence of 500 µmol $L^{-1}$ dopamine. Fig. 4B shows a notorious difference between the magnitude of the anodic (334 mV) and cathodic (44.8 mV) peaks, revealing a greater sensitivity for the oxidation reaction. To estimate the electroactive area, cyclic voltammetry studies were carried out in this configuration, at varying scan rates, ranging from 10 to 200 mV $s^{-1}$, as shown in Fig. S2. Data were applied in the Randles-Sevcik equation, resulting in an electroactive area of 0.22 $cm^2$. Fig. 4C shows the Nyquist diagrams of EIS experiments, performed in presence of 500 µmol $L^{-1}$ dopamine, in 0.1 mol $L^{-1}$ PB solution (pH 6.1), for Gr-AV, as well as the obtained equivalent circuit (Cesiulis et al., 2016), with a $\chi^2$ of 2.84 × $10^{-4}$. The relevant data can be found in the circuit. This experiment implies that the obtained plot contains a superposition of different phases, Gr − AV, Gr − Gr and Gr − dopamine. The proposed electrode based on new conductive ink presented greater resistivity when compared to other published works (Amin et al., 2014; Cinti et al., 2017). Nonetheless, it is valid to observe its adhesion-based nature (Figs. S1B–D). All these characterization data, together, suggest a novel electrochemical device category.

### 3.2. Electrochemical determination of dopamine with Gr-AV disposable electrode

The square ware voltammetry technique was chosen for dopamine detection because of the reversibility of the reaction and its known sensitivity. So, its parameters were studied and optimized, where the selected values were: 8.0 mV for step (*s*), 100 mV for amplitude (*a*) and 10 Hz for frequency (*f*). In addition, tests to evaluate the Gr-AV response in different pHs were carried out, as shows Fig. S3 It was expected that the optimal response would be around pH 7.0 for biological processes; however, a shoulder peak can be observed around 145 mV, which increased in magnitude in more alkaline media, and could be

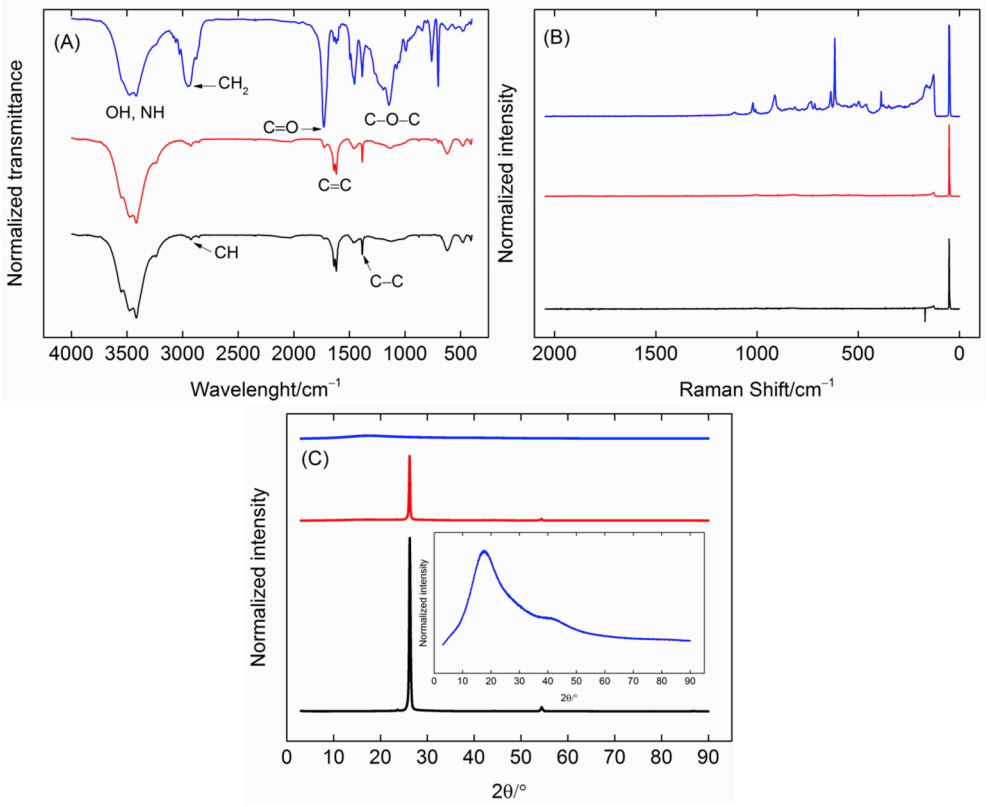


**Fig. 3.** (A) FTIR spectra of automotive varnish (blue line), conductive ink (red line) and graphite powder (black line). (B) Raman spectra of AV (blue), Gr-AV ink (red) and Gr powder (black). (C) X-ray diffraction patterns of AV (blue), Gr-AV ink (red) and Gr (black). Inset shows a closer view of the AV pattern. (For interpretation of the references to color in this figure legend, the reader is referred to the Web version of this article.)

related to the dopamine deprotonation (Breczko et al., 2012; Martínez-Huitle et al., 2009). Therefore, pH 6.1 was chosen as optimal, as it not only presented a better peak resolution, as it also showed less current deviation and no significant peak magnitude was lost.

After the optimization, the analytical curve was constructed for dopamine (oxidation reaction in Fig. S4A), by varying its concentration from 30 to 800 μmol $L^{-1}$, in which was observed an increase in the peak current proportional to the concentration, as presented in Fig. 5A.

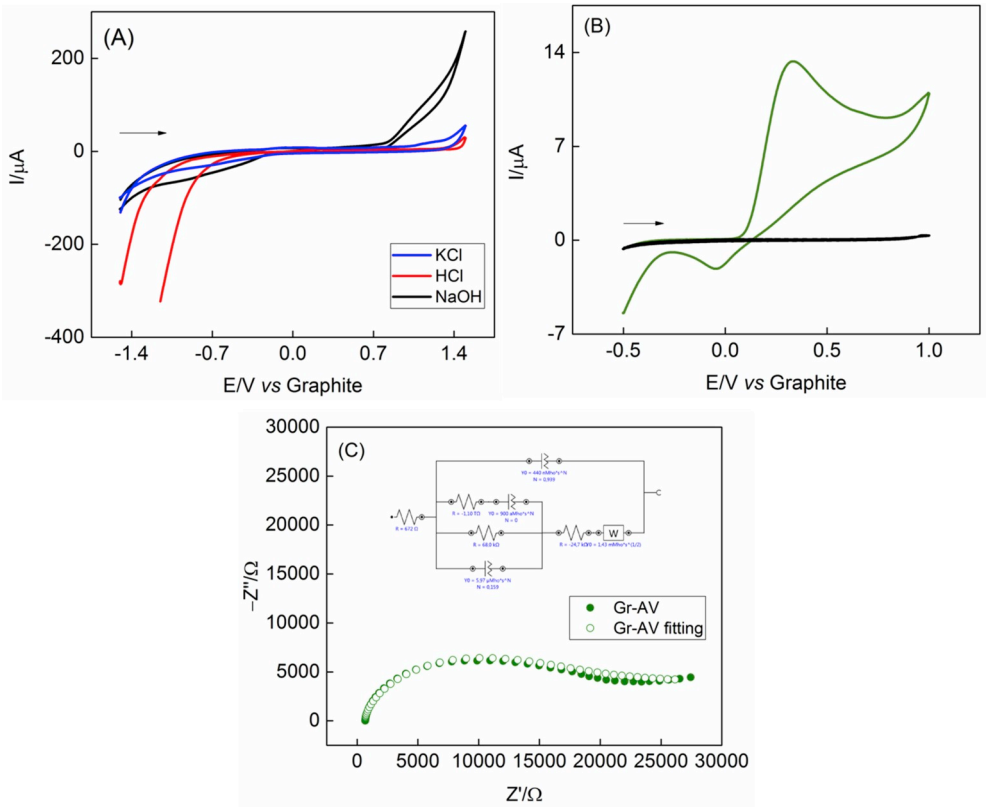


**Fig. 4.** (A) Cyclic voltammograms obtained by Gr-AV in equimolar concentration of 0.1 mol $L^{-1}$ acidic (HCl pH 1.0, red line), alkaline (NaOH pH 13, black line) and neutral media (KCl pH 6.1, blue line); $\nu = 50$ mV $s^{-1}$. (B) Cyclic voltammogram obtained by the disposable adhesive device Gr-AV in presence of 500 μmol $L^{-1}$ dopamine (green) and in absence of it (black), in 0.1 mol $L^{-1}$ PB solution (pH 6.1); $\nu = 50$ mV $s^{-1}$. (C) Nyquist plot of the adhesive device (green) in presence of 500 μmol $L^{-1}$ dopamine, in 0.1 mol $L^{-1}$ PB solution (pH 6.1). Inset shows the equivalent fitting circuit. (For interpretation of the references to color in this figure legend, the reader is referred to the Web version of this article.)

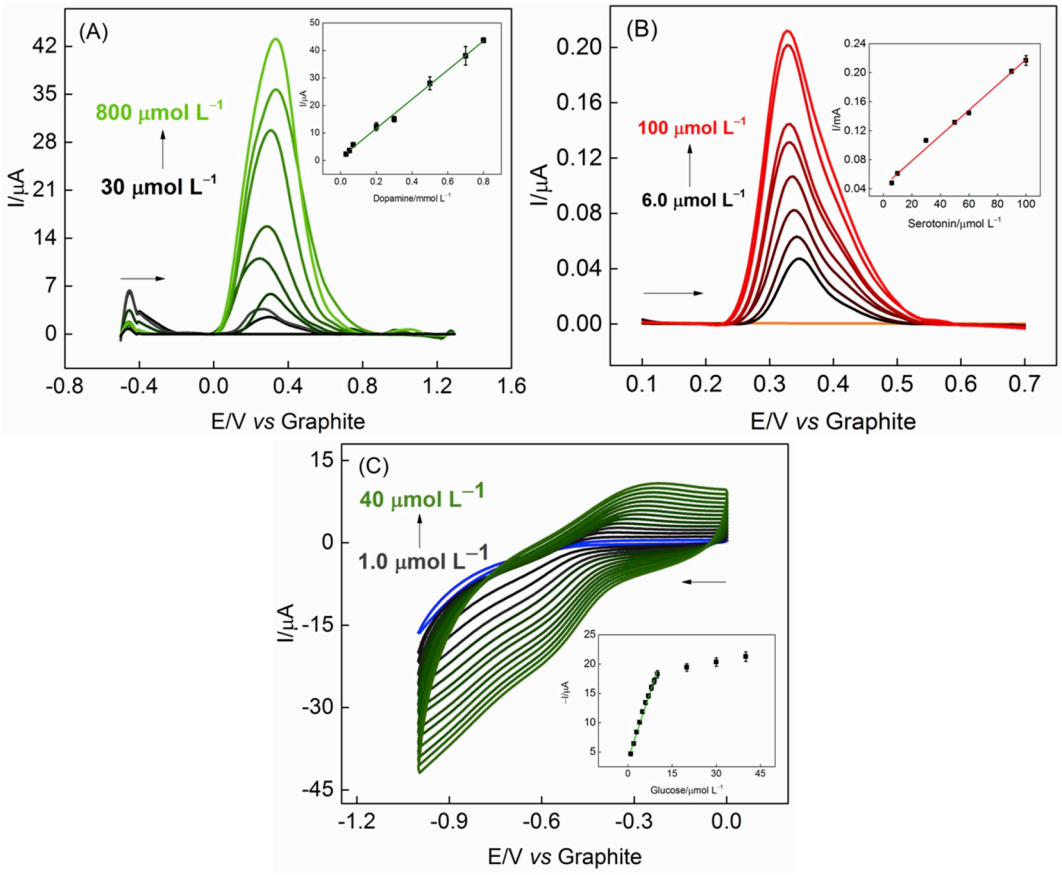


**Fig. 5.** (A) Square ware voltammograms obtained with sticker electrode in presence of different concentrations of dopamine, varying from 30 to 800 µmol $L^{-1}$, in 0.1 mol $L^{-1}$ PB solution (pH 6.1); $s$ = 8 mV; $a$ = 100 mV; $f$ = 10 Hz. Inset shows the analytical curve. (B) Differential pulse voltammograms obtained by Gr-AV in presence of varying concentrations of serotonin, ranging from 0.6 (black) to 100 (lighter red) µmol $L^{-1}$ and in absence of it (orange), in 0.1 mol $L^{-1}$ PB solution (pH 6.1); $v$ = 10 mV $s^{-1}$, $a$ = 25 mV, modulation time = 5 ms. Inset shows the analytical curve. (C) Cyclic voltammograms obtained by GOx-DHP/Gr-AV disposable device in presence of varying glucose concentrations, ranging from 1.0 to 40 µmol $L^{-1}$, in 0.05 mol $L^{-1}$ PB solution (pH 7.0); $v$ = 100 mV $s^{-1}$, $t$ = 60 s. Inset shows the analytical curve. (For interpretation of the references to color in this figure legend, the reader is referred to the Web version of this article.)

**Table 1**
Dopamine and serotonin determinations in spiked saline and synthetic urine samples by Gr-AV; and glucose determination in spiked saline and synthetic saliva samples by GOx-DHP/Gr-AV.

| Gr-AV | | | | | | | |
|---|---|---|---|---|---|---|---|
| DOPAMINE | | | | SEROTONIN | | | |
| Saline | | | | | | | |
| Sample | Added (µmol $L^{-1}$) | Detected (µmol $L^{-1}$) | Recovery% | Sample | Added (µmol $L^{-1}$) | Detected (µmol $L^{-1}$) | Recovery % |
| A | 300 | 305 | 102 | A | 60 | 56 | 93.1 |
| B | 300 | 271 | 90.3 | B | 50 | 52 | 105 |
| C | 800 | 731 | 91.4 | C | 10 | 9.3 | 92.7 |
| Synthetic Urine | | | | | | | |
| A | 30.0 | 26.6 | 83.2 | A | 20 | 22 | 108 |
| B | 50.0 | 51.8 | 104 | B | 30 | 29 | 97.0 |
| C | 70.0 | 76.4 | 109 | C | 90 | 87 | 96.6 |
| GOx-DHP/Gr-AV | | | | | | | |
| GLUCOSE | | | | | | | |
| Saline | | | | Synthetic saliva | | | |
| A | 9.00 | 8.83 | 95.8 | A | 9.00 | 8.83 | 92.1 |
| B | 8.00 | 8.12 | 99.9 | B | 8.00 | 8.12 | 102 |
| C | 7.00 | 7.92 | 103 | C | 7.00 | 7.92 | 113 |

Therefore, it was obtained the linear equation $I_p$ (mA) = $1.05 \times 10^{-6} \pm 5.30 \times 10^{-7} + 0.0530 \pm 1.21 \times 10^{-3}$ $C_{Dopamine}$ (mmol $L^{-1}$) with $R^2$ = 0.997 and the detection limit (LOD) was calculated by three times the standard deviation of the blank divided by the slope of the analytical curve, resulting in a value of 0.13 µmol $L^{-1}$. The Gr-AV electrode was applied for dopamine detection in spiked synthetic urine and saline samples where, respectively, a recuperation ranging from 83.2 to 109% and 90.3–102% was obtained,

as presented in Table 1.

The reproducibility study (four electrodes, one measurement per day, n = 4) was carried out in presence of 500 μmol $L^{-1}$ dopamine, in 0.05 mol $L^{-1}$ PB solution (pH 6.1). The relative standard deviation (RSD) obtained was 4.46%. For the interference study, possible interfering species were used to evaluate the discrepant effects, being carried out with 500 μmol $L^{-1}$ dopamine. In this context, ascorbic (Fig. S5A) and uric (Fig. S5B) acid presented no significant interference (2.0 and 1.0%, respectively) at a concentration of 0.05 mol $L^{-1}$. For creatinine (Fig. S5C), tests with $5.0 \times 10^{-3}$ mol $L^{-1}$ demonstrated an 8.0% peak deviation. However, we highlight that human urinary creatinine concentration ranges from $5.3 \times 10^{-5}$ to $1.1 \times 10^{-4}$ mol $L^{-1}$ (Alessio et al., 1985; Barr et al., 2004; Boeniger et al., 1993). As the concentration is higher than the one found in human urine, it was obtained an acceptable deviation.

### 3.3. Electrochemical determination of serotonin with Gr-AV disposable electrode

To demonstrate the device electroanalytical versatility, Gr-AV was also applied towards the serotonin determination. Tests with cyclic voltammetry, at 50 mV $s^{-1}$, in presence of 100 μmol $L^{-1}$ serotonin, in 0.1 mol $L^{-1}$ PB solution were performed, as shown in Fig. S6. An irreversible anodic peak was observed at 358 mV, with a current magnitude of 0.57 mA, corresponding to the species oxidation (Fig. S4B). Sequentially, a calibration curve was built by differential pulse voltammetry, in order to also demonstrate the device application. A linear behavior was found in the range of 6.0–100 μmol $L^{-1}$, in 0.1 mol $L^{-1}$ PB solution, corresponding to the $I_p(A) = 4.37 \times 10^{-8} \pm 3.90 \times 10^{-9} + 1.75 \times 10^{-3} \pm 6.50 \times 10^{-5}$ $C_{Serotonin}$ (μmol $L^{-1}$) relation, with $R^2 = 0.993$. As aforementioned, the LOD of the sensor was calculated to be 0.39 μmol $L^{-1}$. The corresponding data is present in Fig. 5B. Then, saline solution and synthetic urine samples were spiked with known concentrations of serotonin, in order to evaluate the matrix effect in this case as well. Table 1 presents the recovery data, ranging from 92.7 to 105% for the saline solution and from 96.6 to 108% for the synthetic urine samples.

### 3.4. Electrochemical determination of glucose with the GOx-DHP/Gr-AV disposable electrode

Fig. S7 shows an attempt of detecting 10 μmol $L^{-1}$ glucose with the bare Gr-AV device (red), in 0.05 mol $L^{-1}$ PB solution. As observed, no present component of the sensor can achieve the catalytic effect desired for the glucose reactions (Figs. S4C and D). Therefore, surface modification was evaluated, and the adhesive device was modified with a GOx-DHP dispersion, to obtain an electrocatalytic glucose biosensor. As a surfactant, it is expected (Janegitz et al., 2015) that DHP aqueous dispersions have lipophilic core micelles and hydrophilic heads in contact with the sample solution. In this way, we assure a better wettability, which can improve the electrochemical response (Ibanez-Redin et al., 2018; Ricci et al., 2009; Robinson et al., 2006). Fig. 5C shows cyclic voltammograms obtained with GOx-DHP/Gr-AV in 0.05 mol $L^{-1}$ PB solution (pH 7.0), at $\nu = 100$ mV $s^{-1}$, in increasing concentration of glucose. With the catalyzed consumption of $O_2$, the cathodic baseline decreases linearly to the available glucose, until enzyme site saturation (reactions in Figs. S4C and D). Therefore, all data were collected at 0.6 V and Fig. 5C inset shows the obtained behavior. The system presented linear response in the range of 1.0 μmol $L^{-1}$ to 10 μmol $L^{-1}$, with the equation $I_p(A) = 3.74 \times 10^{-6} \pm 1.82 \times 10^{-7} + 1.52 \pm 0.0536$ $C_{Glucose}$ (μmol $L^{-1}$) and $R^2 = 0.991$. As aforementioned, the LOD of the sensor was calculated to be 0.21 μmol $L^{-1}$. Also, a second linear response can be observed in the range of 10–40 μmol $L^{-1}$ glucose. This considered low sensitivity is due to the effective saturation of enzyme catalytic sites, leading to a detection plateau. Therefore, further additions of glucose would cause an insignificant current variation. The device was applied in the detection of known concentrations of glucose in synthetic saliva and saline samples. For the synthetic saliva, the recovery ranged from 92.1 to 113%, and for the saline samples, from 95.8 to 103%, as shown in Table 1. In order to further evaluate the biosensor, *intradays* (four electrodes, one measurement per electrode, n = 4) and *interdays* (four electrodes, one measurement and electrode per day, n = 4) reproducibility tests were carried out, under optimal conditions, in presence of 5.0 μmol $L^{-1}$ glucose. The calculated RSD values of 2.5 and 7.4% were obtained for *intra* and *interdays*, respectively.

Evaluations of the electrochemical behavior of dopamine in the presence of glucose were also performed by using the proposed electrode. Fig. S5D shows the data of Gr-AV in presence of 500 μmol $L^{-1}$ dopamine and 8.0 μmol $L^{-1}$ glucose, in 0.1 mol $L^{-1}$ PB solution (pH 7.0), at same configurations as the calibration curve for dopamine. Even though the peak presented a large profile, suggesting a slower kinetic effect, the current magnitude does not have significant changes, with an RSD of 1.5% with n = 4. The opposite analysis was carried out with same concentrations, in 0.05 mol $L^{-1}$ PB solution (pH 7.0), by cyclic voltammetry with $\nu = 100$ mV $s^{-1}$ (Fig. S5E) by using the proposed biosensor. A significant alteration can be observed, with RSD of 10%, with n = 4. However, as literature introduces (Bergman et al., 2018; Zen et al., 1997) GOx can interact with dopamine, as many neuronal systems correlate the activities of both analytes. No tests were made in the simultaneous presence of dopamine and serotonin, since both catecholamines have very similar molecular structure and oxidation pattern, and, for this reason, significant influence is expected.

In Table S2, both Gr-AV and GOx-DHP/Gr-AV are compared to others already reported disposable electrochemical devices, towards the detection of dopamine and glucose. The focus was to compare with other disposable sensors, as this is the most commonly equal aspect of this work and the literature. The data demonstrate an equal efficiency between this and other works, validating this approach.

## 4. Conclusions

This work reports the development and application of a novel self-adhesive based electrochemical device, made by conductive ink of Gr and AV, towards the detection of dopamine (from 30 to 800 μmol $L^{-1}$, with a LOD of 0.13 μmol $L^{-1}$), serotonin (from 6.0 to 100 μmol $L^{-1}$, LOD corresponding to 0.39 μmol $L^{-1}$) and glucose (from 1.0 to 10 μmol $L^{-1}$, with a LOD of 0.21 μmol $L^{-1}$) by using three different voltammetric techniques (cyclic; square wave and differential pulse). As proof of concept, these experiments demonstrated acceptable analytical efficiency, with further tests in regards of its reproducibility, possible interfering species and operation in environmental and biological samples, in which both showed promising outcomes in all aspects. This work widens the scope of further surface modification, while simultaneously building interest in the field of electrochemical sensing and biosensing.

## CRediT authorship contribution statement

**Luiz Otávio Orzari:** Conceptualization, Data curation, Formal analysis, Funding acquisition, Investigation, Methodology, Project administration, Resources, Validation, Writing - original draft, Writing - review & editing. **Rafaela Cristina de Freitas:** Conceptualization, Data curation, Formal analysis, Funding acquisition, Investigation, Methodology, Project administration, Resources, Validation, Writing - original draft, Writing - review & editing. **Isabela Aparecida de Araujo Andreotti:** Conceptualization, Data curation, Formal analysis, Funding acquisition, Investigation, Methodology, Project administration, Resources, Validation, Writing - original draft, Writing - review & editing. **Alexandre Gatti:** Conceptualization, Data curation, Formal analysis, Funding acquisition, Investigation, Methodology, Project

administration, Resources, Validation, Writing - original draft, Writing - review & editing. **Bruno Campos Janegitz:** Conceptualization, Data curation, Formal analysis, Funding acquisition, Investigation, Methodology, Project administration, Resources, Validation, Writing - original draft, Writing - review & editing.

## Acknowledgments

The authors acknowledge Fundação de Amparo a Pesquisa do Estado de São Paulo (FAPESP), Brazil (2017/21898–6 and 2016/12697–4), Coordenação de Aperfeiçoamento de Pessoal de Nível Superior (CAPES), Brazil and Conselho Nacional de Desenvolvimento Científico e Tecnológico (CNPq), Brazil for the financial support.

## Appendix A. Supplementary data

Supplementary data to this article can be found online at https://doi.org/10.1016/j.bios.2019.05.015.

## References

Alessio, L., Berlin, A., Dell'Orto, A., Toffoletto, F., Ghezzi, I., 1985. Reliability of urinary creatinine as a parameter used to adjust values of urinary biological indicators. Int. Arch. Occup. Environ. Health 55 (2), 99–106.
Amin, S., Soomro, M.T., Memon, N., Solangi, A.R., Qureshi, T., Behzad, A.R., 2014. Disposable screen printed graphite electrode for the direct electrochemical determination of ibuprofen in surface water. Environ. Nanotechnol. Monit. Manag. 1, 8–13.
Armelin, E., Whelan, R., Martínez-Triana, Y.M., Alemán, C., Finn, M., Díaz, D.D., 2017. Protective coatings for aluminum alloy based on hyperbranched 1, 4-polytriazoles. ACS Appl. Mater. Interfaces 9 (4), 4231–4243.
Arslan, F., Ustabaş, S., Arslan, H., 2011. An amperometric biosensor for glucose determination prepared from glucose oxidase immobilized in polyaniline-poly-vinylsulfonate film. Sensors 11 (8), 8152–8163.
Baccarin, M., Santos, F.A., Vicentini, F.C., Zucolotto, V., Janegitz, B.C., Fatibello-Filho, O., 2017. Electrochemical sensor based on reduced graphene oxide/carbon black/chitosan composite for the simultaneous determination of dopamine and paracetamol concentrations in urine samples. J. Electroanal. Chem. 799, 436–443.
Barr, D.B., Wilder, L.C., Caudill, S.P., Gonzalez, A.J., Needham, L.L., Pirkle, J.L., 2004. Urinary creatinine concentrations in the US population: implications for urinary biologic monitoring measurements. Environ. Health Perspect. 113 (2), 192–200.
Bergman, J., Mellander, L., Wang, Y., Cans, A.-S., 2018. Co-detection of dopamine and glucose with high temporal resolution. Catalysts 8 (1), 34.
Berridge, K.C., Kringelbach, M.L., 2013. Neuroscience of affect: brain mechanisms of pleasure and displeasure. Curr. Opin. Neurobiol. 23 (3), 294–303.
Blackwell, J., Nagarajan, M., Hoitink, T., 1981. Structure of polyurethane elastomers. X-ray diffraction and conformational analysis of MDI-propandiol and MDI-ethylene glycol hard segments. Polymer 22 (11), 1534–1539.
Blair, M., 2016. Diabetes mellitus review. Urol. Nurs. 36 (1), 27–36.
Boeniger, M.F., Lowry, L.K., Rosenberg, J., 1993. Interpretation of urine results used to assess chemical exposure with emphasis on creatinine adjustments: a review. Am. Ind. Hyg. Assoc. J. 54 (10), 615–627.
Breczko, J., Plonska-Brzezinska, M.E., Echegoyen, L., 2012. Electrochemical oxidation and determination of dopamine in the presence of uric and ascorbic acids using a carbon nano-onion and poly (diallyldimethylammonium chloride) composite. Electrochim. Acta 72, 61–67.
Calegari, F., de Souza, L.P., Barsan, M.M., Brett, C.M., Marcolino-Junior, L.H., Bergamini, M.F., 2017. Construction and evaluation of carbon black and poly (ethylene co-vinyl) acetate (EVA) composite electrodes for development of electrochemical (bio) sensors. Sensor. Actuator. B Chem. 253, 10–18.
Campos, A.M., Raymundo-Pereira, P.A., Mendonça, C.D., Calegaro, M.L., Machado, S.A., Oliveira Jr., O.N., 2018. Size control of carbon spherical shells for sensitive detection of paracetamol in sweat, saliva, and urine. ACS Applied Nano Mater. 1 (2), 654–661.
Cesiulis, H., Tsyntsaru, N., Ramanavicius, A., Ragoisha, G., 2016. The Study of Thin Films by Electrochemical Impedance Spectroscopy, Nanostructures and Thin Films for Multifunctional Applications. Springer, pp. 3–42.
Cinti, S., Mazzaracchio, V., Cacciotti, I., Moscone, D., Arduini, F., 2017. Carbon black-modified electrodes screen-printed onto paper towel, waxed paper and parafilm m®. Sensors 17 (10), 2267.
Cryer, P.E., 2016. Chapter 34 - hypoglycemia A2 - melmed, shlomo. In: Polonsky, K.S., Larsen, P.R., Kronenberg, H.M. (Eds.), Williams Textbook of Endocrinology, thirteenth ed. Content Repository Only!, Philadelphia, pp. 1582–1607.
Dunn, D.J., 2003. Adhesives and Sealants Technology, Applications and Markets. Rapra Technology Limited.
Dwier, D.S., 2002. Glucose Metabolism in the Brain.
Fox, S.H., Chuang, R., Brotchie, J.M., 2009. Serotonin and Parkinson's disease: on movement, mood, and madness. Mov. Disord.: official journal of the Movement Disorder Society 24 (9), 1255–1266.
Fukushima, H., Drzal, L., Rook, B., Rich, M., 2006. Thermal conductivity of exfoliated graphite nanocomposites. J. Therm. Anal. Calorim. 85 (1), 235–238.
Ge, S., Ge, L., Yan, M., Song, X., Yu, J., Huang, J., 2012. A disposable paper-based electrochemical sensor with an addressable electrode array for cancer screening. Chem. Commun. 48 (75), 9397–9399.
Goldstein, D.S., 2003. Catecholamines and stress. Endocr. Regul. 37 (2), 69–80.
Grisales, C., Herrera, N., Fajardo, F., 2016. Preparation of graphite conductive paint and its application to the construction of RC circuits on paper. Phys. Educ. 51 (5) 055011.
Ibanez-Redin, G., Silva, T.A., Vicentini, F.C., Fatibello-Filho, O., 2018. Effect of carbon black functionalization on the analytical performance of a tyrosinase biosensor based on glassy carbon electrode modified with dihexadecylphosphate film. Enzym. Microb. Technol. 116, 41–47.
Iversen, L.,L., Iversen, S.D., Snyder, S.H., 1977. In: Handbook of Psychopharmacology, vol. 8 Drugs, Neurotransmitters, and Behavior.
Jaiswal, N., Tiwari, I., 2017. Recent build outs in electroanalytical biosensors based on carbon-nanomaterial modified screen printed electrode platforms. Anal. Methods 9 (26), 3895–3907.
Janegitz, B.C., Baccarin, M., Raymundo-Pereira, P.A., dos Santos, F.A., Oliveira, G.G., Machado, S.A.S., Lanza, M.R.V., Fatibello-Filho, O., Zucolotto, V., 2015. The use of dihexadecylphosphate in sensing and biosensing. Sensor. Actuator. B Chem. 220, 805–813.
Janegitz, B.C., Cancino, J., Zucolotto, V., 2014. Disposable biosensors for clinical diagnosis. J. Nanosci. Nanotechnol. 14 (1), 378–389.
Janegitz, B.C., Pauliukaite, R., Ghica, M.E., Brett, C.M.A., Fatibello, O., 2011. Direct electron transfer of glucose oxidase at glassy carbon electrode modified with functionalized carbon nanotubes within a dihexadecylphosphate film. Sensor. Actuator. B Chem. 158 (1), 411–417.
Johari-Ahar, M., Karami, P., Ghanei, M., Afkhami, A., Bagheri, H., 2018. Development of a molecularly imprinted polymer tailored on disposable screen-printed electrodes for dual detection of EGFR and VEGF using nano-liposomal amplification strategy. Biosens. Bioelectron. 107, 26–33.
Johra, F.T., Lee, J.-W., Jung, W.-G., 2014. Facile and safe graphene preparation on solution based platform. J. Ind. Eng. Chem. 20 (5), 2883–2887.
Kang, W., Pei, X., Rusinek, C.A., Bange, A., Haynes, E.N., Heineman, W.R., Papautsky, I., 2017. Determination of lead with a copper-based electrochemical sensor. Anal. Chem. 89 (6), 3345–3352.
Kent, M.C., Light, N.D., Bailey, A.J., 1985. Evidence for glucose-mediated covalent cross-linking of collagen after glycosylation in vitro. Biochem. J. 225 (3), 745–752.
Khomenko, V., Raymundo-Piñero, E., Béguin, F., 2008. High-energy density graphite/AC capacitor in organic electrolyte. J. Power Sources 177 (2), 643–651.
Lamas-Ardisana, P., Martínez-Paredes, G., Añorga, L., Grande, H., 2018. Glucose biosensor based on disposable electrochemical paper-based transducers fully fabricated by screen-printing. Biosens. Bioelectron. 109, 8–12.
Lee, V.B.C., MOHD-NAIM, N.F., Tamiya, E., Ahmed, M.U., 2018. Trends in paper-based electrochemical biosensors: from design to application. Anal. Sci. 34 (1), 7–18.
Li, L., Reich, S., Robertson, J., 2005. Defect energies of graphite: density-functional calculations. Phys. Rev. B 72 (18), 184109.
Martínez-Huitle, C.A., Cerro-Lopez, M., Quiroz, M.A., 2009. Electrochemical behaviour of dopamine at covalent modified glassy carbon electrode with l-cysteine: preliminary results. Mater. Res. 12 (4), 375–384.
Mayeux, R., Stern, Y., Cote, L., Williams, J.B., 1984. Altered serotonin metabolism in depressed patients with Parkinson's disease. Neurology 34 (5) 642-642.
Mittal, K.L., 2003. Adhesion Aspects of Polymeric Coatings. VSP BV.
Naumenko, A., Yashchuk, V., Bliznyuk, V., Singamaneni, S., 2012. Peculiarities of Raman spectra of polyurethane/carbon nanotube composite. Euro. Phys. J. B 85 (4), 120.
Negash, N., Alemu, H., Tessema, M., 2015. Electrochemical characterization and determination of phenol and chlorophenols by voltammetry at single wall carbon nanotube/poly(3,4-ethylenedioxythiophene) modified screen printed carbon electrode. Int. Scholarly Res. Not. 459246 2015.
Orzari, L.O., de Araujo Andreotti, I.A., Bergamini, M.F., Junior, L.H.M., Janegitz, B.C., 2018. Disposable electrode obtained by pencil drawing on corrugated fiberboard substrate. Sensor. Actuator. B Chem. 264, 20–26.
Ozawa, K., Hashimoto, K., Kishimoto, T., Shimizu, E., Ishikura, H., Iyo, M., 2006. Immune activation during pregnancy in mice leads to dopaminergic hyperfunction and cognitive impairment in the offspring: a neurodevelopmental animal model of schizophrenia. Biol. Psychiatry 59 (6), 546–554.
Parnell, S., Min, K., Cakmak, M., 2003. Kinetic studies of polyurethane polymerization with Raman spectroscopy. Polymer 44 (18), 5137–5144.
Pekarovicova, A., Fleming, P.D., 2005. Innovations in Ink and Paper Technology to Improve Printability. Pira international Ltd.
Phillips, C., Al-Ahmadi, A., Potts, S.-J., Claypole, T., Deganello, D., 2017. The effect of graphite and carbon black ratios on conductive ink performance. J. Mater. Sci. 52 (16), 9520–9530.
Pierson, H.O., 2012. Handbook of Carbon, Graphite, Diamonds and Fullerenes: Processing, Properties and Applications. William Andrew.
Pisoschi, A.M., 2012. Glucose determination by biosensors. Biochem. Anal. Biochem. 1, 1–2.
Popova, A.N., 2017. Crystallographic analysis of graphite by X-Ray diffraction. Coke Chem. 60 (9), 361–365.
Pradhan, K.C., Nayak, P., 2012. Synthesis and characterization of polyurethane nanocomposite from castor oil-hexamethylene diisocyanate (HMDI). Adv. Appl. Sci. Res. 3 (5), 3045–3052.
Purushothama, H.T., Nayaka, Y.A., Vinay, M.M., Manjunatha, P., Yathisha, R.O., Basavarajappa, K.V., 2018. Pencil graphite electrode as electrochemical sensor for the voltammetric determination of chlorpromazine. J. Sci.: Adv. Mater. Dev. 3 (2), 161–166.
Raymundo-Pereira, P.A., Shimizu, F.M., Coelho, D., Piazzeta, M.H., Gobbi, A.L., Machado, S.A., Oliveira Jr., O.N., 2016. A nanostructured bifunctional platform for

sensing of glucose biomarker in artificial saliva: synergy in hybrid Pt/Au surfaces. Biosens. Bioelectron. 86, 369–376.
Ricci, F., Zari, N., Caprio, F., Recine, S., Amine, A., Moscone, D., Palleschi, G., Plaxco, K.W., 2009. Surface chemistry effects on the performance of an electrochemical DNA sensor. Bioelectrochemistry 76 (1–2), 208–213.
Robinson, L., Isaksson, J., Robinson, N.D., Berggren, M., 2006. Electrochemical control of surface wettability of poly(3-alkylthiophenes). Surf. Sci. 600 (11), L148–L152.
Schultz, W., 2001. Reward signaling by dopamine neurons. Neuroscientist : a review journal bringing neurobiology, neurology and psychiatry 7 (4), 293–302.
Sharma, S., Singh, N., Tomar, V., Chandra, R., 2018. A review on electrochemical detection of serotonin based on surface modified electrodes. Biosens. Bioelectron. 107, 76–93.
Sharp, D., Burkitt, R., 2015. Carbon materials for analytical electrochemistry: printed carbon materials and composites. Mater. Technol. 30 (Suppl. 7), B155–B162.
Smith, A., 1982. In: The Coblentz Society Desk Book of Infrared Spectra The Coblentz society desk book of infrared spectra, pp. 1–24.
Steinbusch, H., Verhofstad, A., Joosten, H., 1978. Localization of serotonin in the central nervous system by immunohistochemistry: description of a specific and sensitive technique and some applications. Neuroscience 3 (9), 811–819.
Syedmoradi, L., Daneshpour, M., Alvandipour, M., Gomez, F.A., Hajghassem, H., Omidfar, K., 2017. Point of care testing: the impact of nanotechnology. Biosens. Bioelectron. 87, 373–387.
Tian, X., Itkis, M.E., Bekyarova, E.B., Haddon, R.C., 2013. Anisotropic thermal and electrical properties of thin thermal interface layers of graphite nanoplatelet-based composites. Sci. Rep. 3, 1710.
Tortorich, R., Shamkhalichenar, H., Choi, J.-W., 2018. Inkjet-printed and paper-based electrochemical sensors. Appl. Sci. 8 (2), 288.
Vyazovskiy, V.V., Riedner, B.A., Cirelli, C., Tononi, G., 2007. Sleep homeostasis and cortical synchronization: II. A local field potential study of sleep slow waves in the rat. Sleep 30 (12), 1631–1642.
Wang, H.-C., Lee, A.-R., 2015. Recent developments in blood glucose sensors. J. Food Drug Anal. 23 (2), 191–200.
Wang, P., Wang, M., Zhou, F., Yang, G., Qu, L., Miao, X., 2017. Development of a paper-based, inexpensive, and disposable electrochemical sensing platform for nitrite detection. Electrochem. Commun. 81, 74–78.
Xu, G., Jarjes, Z.A., Desprez, V., Kilmartin, P.A., Travas-Sejdic, J., 2018. Sensitive, selective, disposable electrochemical dopamine sensor based on PEDOT-modified laser scribed graphene. Biosens. Bioelectron. 107, 184–191.
Xu, L., Li, C., Ng, K.S., 2000. In-situ monitoring of urethane formation by FTIR and Raman spectroscopy. J. Phys. Chem. A 104 (17), 3952–3957.
Zarei, M., 2017. Portable biosensing devices for point-of-care diagnostics: recent developments and applications. Trac. Trends Anal. Chem. 91, 26–41.
Zen, J.-M., Lo, C.-W., Chen, P.-J., 1997. An enzymatic clay-modified electrode for aerobic glucose monitoring with dopamine as mediator. Anal. Chem. 69 (8), 1669–1673.